Photodiagnosis and Photodynamic Therapy 25 (2019) 119–127

Contents lists available at ScienceDirect

Photodiagnosis and Photodynamic Therapy

journal homepage: www.elsevier.com/locate/pdpdt

Adipogenic differentiation of murine bone marrow mesenchymal stem cells induced by visible light via photo- induced biomodulation

Andrielle Castilho-Fernandes[a], Tácila G. Lopes[a], Fernanda U. Ferreira[b], Nayara Rezende[a], Valéria F. Silva[a,b], Fernando L. Primo[a,d], Aparecida Maria Fontes[e], Alfredo Ribeiro-Silva[c], Antonio Claudio Tedesco[a,*]

[a] Department of Chemistry, Center of Nanotechnology and Tissue Engineering – Photobiology and Photomedicine Research Group, Faculty of Philosophy, Sciences and Letters of Ribeirão Preto, Ribeirão Preto, University of São Paulo, 14040-901, Brazil
[b] Center for Cell Therapy and Regional Blood Center, National Institute of Science and Technology in Stem Cell and Cell Therapy, Medical School, University of São Paulo, Ribeirão Preto 14051-140, Brazil
[c] Department of Pathology, Medical School, University of Sao Paulo, Ribeirao Preto 14049-900, Brazil
[d] Departament of Bioprocess and Biotechnology, São Paulo State University (UNESP), School of Pharmaceutical Sciences, Araraquara SP 14800-903, Brazil
[e] Departament of de Genetics, Medical School, University of São Paulo, Ribeirão Preto 14051-140, Brazil

ARTICLE INFO

Keywords:
Bone marrow-mesenchymal stem cells (BM-MSC)
Photo induced biomodulation
Low level laser (LLL)
Chloroaluminum phthalocyanine (AlClPc)
Adipogenic differentiation

ABSTRACT

Background: Bone marrow mesenchymal stem cells (BM-MSCs) are undifferentiated cells that can proliferate and differentiate into specialized cells for tissue self-repair. Low-level laser (LLL) can induce biomodulatory effects such as cellular proliferation, differentiation, and migration. We investigated the biomodulatory effects of the photoactive compound chloroaluminum phthalocyanine nanoemulsion (AlClPc/NE) on the adipogenic differentiation of BM-MSCs, when combined with LLL (AlClPc/NE-LLL).

Methods: The BM-MSCs used in this work were isolated from green fluorescent protein-positive (GFP^+) C57BL6 mice. Cells were first treated with AlClPc/NE, a well-designed photoactive nano-drug and were then subjected to *in vitro* expansion, morphological and immunophenotypic characterization, and cellular cytotoxicity analysis. Subsequently, BM-MSCs were induced to differentiate into adipocytes by photo-induced biomodulation with AlClPc/NE-LLL.

Results: Our results showed that the isolated cell population was consistent with murine BM-MSCs. The cellular cytotoxicity analysis revealed that the optimal nanoemulsion dose to induce BM-MSC biomodulation was 5.0 μmol/L. Twenty-four hours following treatment with AlClPc/NE, BM-MSC were subjected to visible light irradiation of 20 mJ/cm^2 at 670 nm. Six days after photo-induced biomodulation, cells maintained high GFP expression level, and expressed detectable mRNA levels of adipogenic genes (lipoprotein lipase and PPARγ); formation of lipid vacuoles was observed, and the cells did not show any tumorigenic potential *in vivo*.

Conclusions: Our results indicated that photo-induced biomodulation via visible light using AlClPc/NE and LLL can induce adipogenic differentiation of murine BM-MSCs. Therefore, cell therapy with BM-MSCs and photo-induced biomodulation may contribute to the development of new therapeutic strategies that are faster and more effective than traditional methods to trigger MSC differentiation.

1. Introduction

Mesenchymal stem cells (MSCs) are multipotent cells that are isolated from bone marrow (BM-MSCs), and exhibit fibroblast-like morphology [1]. BM-MSCs are capable of extensive self-renewal without malignant changes and can differentiate into cells of different lineages. Thus, they hold promise for many clinical applications [2]. MSCs may be used to repair damaged tissue, such as in reconstructive surgeries [3,4]. MSCs exhibit immunomodulatory properties, as these do not cells express costimulatory molecules or major histocompatibility complex (MHC) class II and do not trigger immune responses in allogeneic recipients [5].

The MSC lineage has been shown to be sensitive to biophysical and biochemical properties of the extracellular matrix, such as the type of adhesion ligands that are present in the microenvironment [6]. Therefore, extensive studies have been conducted on MSC isolation,

* Corresponding author.
E-mail address: atedesco@usp.br (A.C. Tedesco).

https://doi.org/10.1016/j.pdpdt.2018.11.013
Received 24 June 2018; Received in revised form 13 November 2018; Accepted 16 November 2018
Available online 17 November 2018

culture, and differentiation. While there is now greater understanding of MSC biology, and its availability has increased, an alternative method for adipogenic differentiation of BM-MSCs that is faster and more reliable is still lacking. In 2011, Cristancho and Lazar reported that adipogenesis proceeds in two stages. The first stage is known as pre-adipocytic differentiation; during this time period, MSCs are regulated by biophysical and biochemical signals such as cell shape and matrix ligands. The second stage is known as terminal differentiation, were adipocytes mature upon activation of peroxisome proliferator-activated receptor γ (PPARγ) [7].

Adipogenic differentiation of MSCs has generated much interest among researchers in many areas of medicine. From a clinical point of view, physicians need to face challenging reconstructive cases, such as soft tissue resorption [8]. For instance, human immunodeficiency virus (HIV)-infected patients that use highly active antiretroviral therapy develop facial lipodystrophy, which can become an aesthetic problem [9]. Additionally, burn patients also often experience soft tissue atrophy [10]. These patients may benefit from tissue engineering for reconstruction of adipose tissues via regenerative medicine. Thus, it is necessary to develop faster and more reliable methods for triggering adipogenic differentiation of BM-MSCs.

Studies have shown that the higher the proliferation rates of MSCs, the greater is the regenerative and healing capacity of the tissues they reside in. Within this context, low-level laser (LLL) irradiation has been shown to be effective in a variety of medical conditions such as mucosal healing, skin ulcers, dermatitis, and mucositis by exerting positive biomodulatory effects on MSCs [11]. Photo-induced biomodulation is achieved through visible light sources with low power, such as light-emitting diodes (LEDs), low-level laser light (LLL), or light emitters in the visible red to near-infrared (NIR) region [12]. However, the underlying molecular mechanisms of this process are not completely understood. It has been suggested that the energy of the laser is absorbed by intracellular chromophores, and is converted into metabolic energy, which is then used by the mitochondrial respiratory chain to produce ATP; this enhances DNA activity and synthesis of RNA and proteins [11]. Thus, the effective of the energy absorbed by the laser would be highly significant. One such mechanism is photodynamic therapy (PDT). PDT involves the transfer of energy from a photosensitizer that absorbs visible light to molecular oxygen, which results in generation of excited state singlet oxygen [13]. Studies have shown associations between the epidermal growth factor receptor (EGFR) pathway and PDT cancer stem cells cytotoxicity [13,14]. LLL is widely used for tissue regeneration, especially to stimulate growth of osteoblasts [15]. Studies have shown that combination therapy based on MSCs and low-level laser irradiation may yield positive results in therapeutic approaches [16].

Chloroaluminum phthalocyanine (AlClPc) has been used as a photosensitizer (PS) in various nano-drug delivery systems in the form of a nanoemulsions (AlClPc/NE). It can be excited by visible light (660 nm), and has demonstrated clinical effectiveness in skin cancer therapy (based by PDT) or wound healing process [17,18]. Kushibiki et al. (2015) demonstrated that multipotent stem cells can differentiate into osteoblasts with LLL doses above 3 J/cm^2 [19]. In addition, our group has shown that LLL irradiation can effectively promote photo-induced biomodulation of osteoblast cell cultures [20]. Nonetheless, the differentiation of BM-MSCs into adipocytes or biomodulation of adipocyte growth by means of LLL has not been elucidated.

Therefore, in this study, we investigated the photo-induced biomodulatory effects of AlClPc/NE and visible range LLL (AlClPc/NE-LLL) on the differentiation of BM-MSCs into adipocytes. We hypothesized that a low concentration of AlClPc/NE combined with LLL may trigger cellular proliferation and differentiation without significant cytotoxicity. This may improve adipogenic differentiation of BM-MSCs and enhance regenerative protocols in the future.

2. Materials and methods

2.1. Animals

C57BL/6-GFP$^+$ mice were provided by Biotery II from the School of Pharmaceutical Sciences of Ribeirão Preto, University of São Paulo, Brazil. Mice in all the experiments were 6–8 weeks old, and weighed 25–30 g. All animals were maintained at temperatures between 21–23 °C, and were kept on a 12-h light–dark cycle. All the experiments were approved by the local administrative authority; animals received care in accordance to guidelines provided by the Ethics Committee on Animal Use of the Faculty of Medicine of Ribeirao Preto, University of São Paulo (CEUA of the *Campus* of Ribeirão Preto – USP, under protocol number 11.1.1332.53.0).

2.2. Isolation and expansion of cells

C57BL/6-GFP$^+$ male mice were sacrificed by cervical dislocation; the femurs, humeri, and tibiae were carefully cleaned from the adherent soft tissues. BM-MSCs were harvested by inserting a 23-gauge syringe needle into one end of the bone, followed by flushing with 10% PBS at pH 7.2. Cells were centrifuged in Eppendorf tubes at 1200 rpm for 10 min, after which they were resuspended in Minimum Essential Medium, Alpha Modification (αMEM), supplemented with 15% foetal bovine serum (FBS), 100 μg/mL penicillin, and 100 U/mL streptomycin. Cells were seeded into 75-cm^2 tissue culture flasks, and were cultured in a humidified incubator at 37 °C and 5% CO_2 for 72 h. Non-adherent cells were removed by washing with PBS (1×), and the medium was changed. When cultures reached 80–90% confluence, sub-culturing was performed; the split ratio was 1:4. The culture medium was changed every 3–4 days.

2.3. Flow cytometric analysis of immunophenotype

The immunophenotypic characterization of BM-MSCs was performed by flow cytometry. Cells were dissociated with trypsin and EDTA and washed twice with 10% PBS. Cell pellets were diluted with PBS and incubated with a phycoerythrin (PE)-conjugated rat anti-mouse or allophycocyanin (APC)-conjugated rat anti-mouse IgG antibodies (1 μg per 10^6 cells) at room temperature for 30 min. Cells were then washed twice with PBS and stained with 1 μg of propidium iodide prior to analysis. Primary antibodies were specific for surface antigens CD73 (PE conjugate), CD44 (APC conjugate), CD117 (APC), CD105 (PE), Sca-1 (APC), CD34 (PE), CD31 (APC), CD45 (APC), and CD11b (PE) (BD Pharmingen). Cells were also stained with the APC- or PE-labelled rat anti-mouse IgG antibody, which served as negative controls. Cells were pelleted by centrifugation, washed twice with PBS, and fixed with 1% paraformaldehyde in 1 × PBS. Fluorescence-activated cell sorting (FACS) analysis was performed on a FACSCalibur flow cytometer (BD Biosciences). Ten thousand events were acquired, and analysis was conducted with the *CellQuest* software (BD Biosciences).

2.4. Morphological analysis and imaging

BM-MSC cultures were routinely examined under an inverted phase contrast microscope (Zeiss). Images were captured with a digital camera (AxioCam; Zeiss) coupled to an inverted microscope (AxioVert; Zeiss), using the AxioVision 3.1 software (Zeiss).

2.5. Nanostructured system preparation: NE

Preparation of NEs, either empty or with AlClPc, was carried out according to the modified protocol described by Primo et al. (2008). The spontaneous emulsification oil in water (o/w) process [21], as previously described by Tabosa do Egito et al. (1993) [22] was used, followed by the interfacial deposition of photoactive drugs. Briefly, an

organic phase with spectroscopic-grade acetone containing phospholipids Epikuron® 170/Span 80® (Lucas Meyer, France/Aldrich) was prepared. AlClPc (Sigma-Aldrich) was pre-dissolved in Miglyol 812 N (Stallergenes S.A.) and was added to the organic solution; this was slowly injected into the aqueous phase containing Poloxamer 188 (ICI), with magnetic stirring. The organic solvent was removed by evaporation under reduced pressure, as previously described [21].

2.6. Cytotoxicity assay of AlClPc/NE in the dark

To assess the intrinsic cytotoxic effect of AlClPc/NE, BM-MSCs were seeded at 10^3 cells/well in a 96-well plate. After 24 h, BM-MSCs were incubated with fresh medium with AlClPc/NE at final concentrations of 0.5, 1.0, 2.5, 5.0, or 7.5 μmol/L^{-1} at 37 °C and 5% CO_2 for 3 h in the dark. Following the incubation period, the medium containing the NE dispersion was discarded. Cells were washed twice with 10% PBS, followed by incubation in fresh medium for an additional 24 h; cell viability was assessed via MTT. Control cells were incubated with the culture medium alone (no-treatment group) or with the nano-emulsion without AlClPc in the dark. Experiments were carried out in triplicates, and 16 wells were used for each AlClPc/NE concentration.

2.7. The MTT assay

The MTT cell proliferation assay [23] assesses cell viability after cytotoxic or photo-cytotoxic assays. Briefly, 80 μL of the MTT solution (5 mg mL^{-1}) and 420 μL of the medium without phenol red were added to each well. Cells were then incubated at 37 °C and 5% CO_2 for 4 h for the formazan-forming reaction to proceed. Following incubation, the medium was removed, and the formazan crystals were dissolved in 2-propanol. Optical density was measured at 570 and 690 nm using a Safire^2 microplate reader (TECAN Group Ltd.). Results were presented as the percentage of cell survival relative to negative control (untreated cells).

2.8. AlClPc/NE-LLL-induced adipogenic differentiation

To investigate the possible photo-induced biomodulatory effect of AlClPc/NE-LLL on adipogenic differentiation of BM-MSCs *in vitro*, cells were seeded at 10^4/well in 6-well plates. After 24 h, BM-MSCs were treated with medium containing AlClPc/NE at 2.5 or 5.0 μmol/L^{-1} (5% CO_2, 37 °C) for 3 h. The medium was removed, and cells were rinsed twice with PBS, followed by incubation in fresh medium for an additional 24 h. For photo-induced biomodulation assays, fresh medium without phenol red was added, and cells were irradiated with a diode Eagle laser (Quantum Tech) at 660 nm; average power was 100 mW, with an irradiance of 14 mW/cm^2. Cells were exposed to light doses at 20 and 40 mJ/cm^2. The parameters used in the present experiment are shown in Table 1. After irradiation, the colourless medium was removed, and cells were incubated (5% CO_2, 37 °C) in fresh medium; the medium was changed two times per week. Control cells were incubated with the culture medium alone without irradiation (no-treatment control), or with AlClPc/NE without irradiation (AlClPc/NE control). Medium alone with LLL (LLL control) served as negative control. All assays were carried out in triplicate. BM-MSCs were analysed every day, and adipocytes were easily distinguished from undifferentiated cells via phase-contrast microscopy. Sudan II-Scarlet staining (Oil Red O; Sigma-Aldrich) was applied to better visualize lipid-rich vacuoles.

Table 1
Parameters used in the low-level laser experiment.

	20 mJ/cm^2	40 mJ/cm^2
Power (W)	0.05	0.05
6-well plates, well diameter (cm)	3.4	3.4
Irradiation time (s)	15	15
Irradiance (mW/cm^2)	1	1
Energy (J)	0.75	1.50
Time (sec)	15	30
Wavelength (nm)	650	650

*Parameters of low laser irradiation were adjusted when using 24-well plates (1.5 cm diameter wells).

2.9. Cytotoxicity assay of adipogenic differentiation induced by AlClPc/NE-LLL

To assess the possible intrinsic photo-cytotoxic effect of AlClPc/NE-LLL on adipogenic differentiation, BM-MSCs were seeded at 10^3 cells/well in 24-well plates, and AlClPc/NE-LLL adipogenic differentiation was conducted as described above. After BM-MSCs were subjected to AlClPc/NE-LLL, cells were incubated with fresh medium for growth curve analyses (1–7 days) by MTT. Control cells (no-treatment group) and adipocytes (experimental group) were incubated with fresh culture medium. Experiments were carried out in triplicates.

2.10. Conventional adipogenic differentiation assays

BM-MSCs were tested for their potential to differentiate into adipocytes by induction. Cells from each source (10^4) were seeded on glass coverslips (GoldLabl) in 24-well plates (Corning) and were incubated with the conventional differentiation medium. For adipogenic differentiation, cells were grown in α-MEM (Gibco-Invitrogen) supplemented with 15% FBS (Thermo Scientific HyClone), 1 mM dexamethasone (Sigma-Aldrich), 2.5 mg/mL insulin, and 0.5 mM isobutylmethylxanthine (Sigma-Aldrich). Sudan II-Scarlet staining (Oil Red O; Sigma-Aldrich) was used to visualize lipid-rich vacuoles. Control groups were cultured in standard α-MEM (Gibco-Invitrogen) with 15% FBS (Thermo Scientific HyClone) in the same period. The cells were analysed with an AxioScope equipped with an AxioCam HR (Carl Zeiss).

2.11. RNA isolation and cDNA synthesis

Total RNA was extracted from BM-MSCs with the RNeasy Mini kit (Qiagen) and stored at −80 °C. RNA was quantified using a NanoVue system (GE Healthcare). RNA quality was determined by assessing the integrity of the 28S and 18S rRNA bands on a 1% agarose gel. Complementary DNA (cDNA) was synthesized from 2 μg total RNA with a High Capacity cDNA Archive Kit (Applied Biosystems).

2.12. qPCR analysis

Gene expression levels of peroxisome proliferator-activated receptors (PPARγ), lipoprotein lipase (LPL), and green fluorescent protein (GFP) were assessed in control and treated BM-MSCs. Quantitative real-time PCR (qPCR) [27] was conducted in 15 μL reaction mixtures for 40 cycles using universal cycling conditions (40 cycles at 95 °C for 15 s; 60 °C for 1 min) on an ABI Prism 7500 Sequence Detection System (Applied Biosystems); SYBR® Green PCR Master Mix with efficiency values between 1.22–0.93 and TaqMan® Universal PCR Master Mix (Applied Biosystems) were used. Concentrations of SYBR primers were 2.5 μM. Gene expression was normalized to that of *GAPDH*, and relative gene expression levels in the different cells types were determined as described previously [24]. cDNAs were diluted 5-fold with nuclease-free H_2O for all qPCR reactions. The sequences of SYBR green primers (forward/reverse) were: LPL F, 5′-CTTTTCTGGGACTGAGGATG and R-, 5′−CCGTGTAAATCAAGAAAGGAGT; PPARγ F 5′-ACATAAAGTCCTTC CCGCTG and R 5′-GGGTGATATGTTTGAACTTGAT; and GFP F 5′-CAC CATCTTCTTCAAGGACG and R 5′-GTGCTCAGGTAGTGGTTGTC.

2.13. In vivo tumorigenic assay tumorigenic assay

Approximately 10^6 BM-MSCs were resuspended in 200 μL sterile

PBS, and were injected subcutaneously (sc) into the dorsal midline of three mice (C57BL/6-GFP$^+$) with a 25-gauge needle attached to a 1-mL syringe (BD Bioscience). Injected mice were monitored daily for appearance of palpable tumours. As experimental controls, PBS-only and BM-MSC-only were injected sc into female mice. After 21 days, all animals were euthanised for examination of tumour formation.

2.14. Histological examination

Tissue samples (BM-MSCs subjected or not subjected to adipogenic differentiation induction with AlClPc/NE-LLL) were fixed in 3.7% formaldehyde for at least 24 h. Next, tissue samples were dehydrated in serial ethanol/xylene dilutions, embedded in paraffin blocks, and sectioned to 5-μm thickness. Tissue sections were stained with haematoxylin-eosin (H&E) for histopathologic analysis under a light microscope (AxioScope) equipped with an AxioCam HR (Carl Zeiss).

2.15. Statistical analysis

Assays were conducted on cells isolated from at least three mice (from the bone marrow) and were carried out in triplicate. To evaluate differences between control and experimental group after induction of adipogenic differentiation, we used ANOVA followed by Tukey's multiple comparison test. Results were expressed as mean ± standard deviation (SD). $P < 0.05$ was considered to be significant. All statistical analyses were conducted with the GraphPad Prism 7.0 software (La Jolla).

3. Results

3.1. Isolation and characterization of murine BM-MSCs

BM-MSCs were isolated from the bone marrow cavity of C57BL/6-GFP$^+$ mice (n = 8); the marrow was flushed out with 1 × PBS. BM-MSCs were seeded in 75-cm^2 tissue culture flasks (Fig. 1A–C) and were cultured for 7–10 days (Fig. 1D). During the first medium change after 48 h (Day 2), non-adherent cells were carefully discarded along with the old medium, and 10 mL of fresh medium was added (Fig. 1C). Some fibroblast-like cells were attached to the flask, and were observed 48–72 h after initial cultivation (Fig. 1C and D). Accordingly, adherent cells {passage 0 (P0)} were washed with PBS (1 ×), and the medium was refreshed every 3 days. Adherent cells gradually grew and formed cellular isolate colonies with fibroblast-like morphology with short and long processes. Adherent fibroblast-like cells became more confluent (Fig. 1D) and reached 80% confluence within 7–10 days. After the second trypsinization {passage 2 (P2)}, BM-MSCs began to grow homogeneously, and fibroblast-like cells occupied the entire plastic surface (Fig. 1E). BM-MSCs were reseeded under the same conditions for the next passages. At P4 (passage 4), non-adherent cells were entirely eliminated, and BM-MSCs were deemed ready for experimentation (Fig. 1F).

To analyse the immunophenotype of isolated cells at P4, murine surface markers were probed by flow cytometry. Accordingly, isolated cells showed murine MSC-specific markers, including CD73 (64.1% ± 9.5% of all cells), CD44 (21.2% ± 8.9%), CD117 (28.2% ± 7.3%), and CD105 (26.1% ± 11%). Sca-1 is the most reliable murine BM-MSC marker and was strongly expressed (90.9% ± 4%). The classical hematopoietic stem cell markers CD31 (0.63% ± 0.4%), CD11b (0.24% ± 0.3%), and CD34 (3% ± 1.6%), as well as the endothelial marker CD45 (20.7% ± 9.4%) were not expressed or were only detectable in a small proportion of cells (Table 2). The expression patterns of murine BM-MSC surface markers suggested that the isolated murine BM-MSCs were typical murine MSCs (Fig. 2).

To evaluate the adipogenic potential of murine BM-MSCs, we subjected the cells (obtained at P4) to adipogenic differentiation. After 14 days of culturing in the conventional adipogenic-differentiation inducer medium, BM-MSCs showed adipogenic characteristics such as acquisition of intracellular lipid droplets, as evidenced by Sudan II/Scarlet staining (Fig. 3J). This was not observed in control BM-MSCs (Fig. 3E). These results further confirmed expression of murine BM-MSC-like

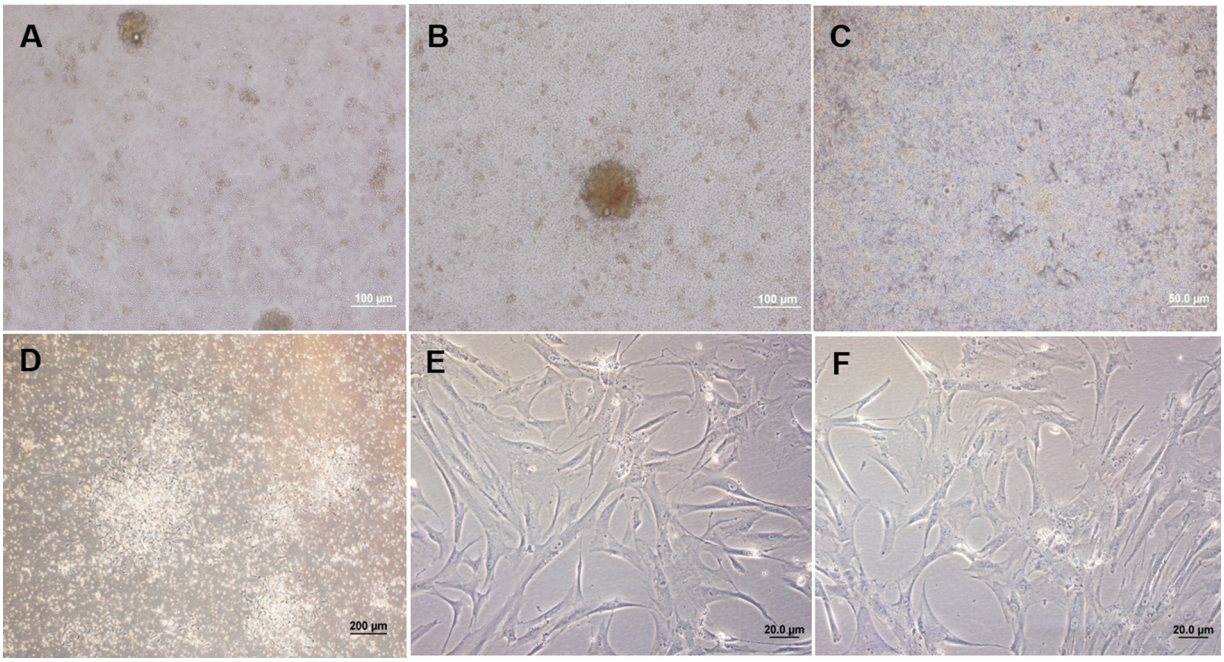

Fig. 1. Cell culture of isolated primary murine BM-MSCs Images were taken using an inverted phase-contrast microscope. P0 of BM-MSCs (panels A–D). Day 0 (panel A) and day 1 (panel B) showed several non-adherent cells in the culture medium. On day 2 a few adherent fibroblast-like cells that began attaching to plastic dish were observed (panel C). Day 4, the non-adherent cells were eliminated by washing with a PBS (1X) and fresh α-MEM medium supplemented with 15% FBS (panel D). P2, second process of trypsinization, cells were plastic-adherent with a spindle-shaped morphology and began to growth in a homogeneous manner (panel E). P4, fourth process of trypsinization, nonadherent cells are totally eliminated, BM-MSCs occupied the whole plastic surface and were ready to be submitted to the experimental studies (panel F). The scale bars represent 20 μm (panels E and F), 50 μm (panel C), 100 μm (panels A and B) and 200 μm (panel D).

Table 2
AlClPc/NE-LLL changes the mesenchymal immunophenotypic profile of experimental group of BM-MSCs. Percentage data presented is the mean ± SD of triplicate cultures.

Surface Markers	*No treatment Control Group*	*LLL Control Group*	*AlClPc/NE Control Group*	*AlClPc/NE-LLL Experimental* Group
CD73	64.1 ± 9.5	59.8 ± 16.9	62.5 ± 2.2	5.9 ± 6.1
CD44	21.2 ± 8.9	51.7 ± 5.6	27 ± 14.9	10.9 ± 10.1
CD117	28.2 ± 7.3	7.8 ± 4.5	14.7 ± 7.2	2.2 ± 0.6
CD105	26.1 ± 11	16 ± 10.3	5.4 ± 2.3	2.8 ± 1.1
SCA 1	90.9 ± 4	97.9 ± 2.7	81.9 ± 17.8	79.8 ± 17.6
CD34	3.0 ± 1.6	2.0 ± 0.9	2.0 ± 1.2	1.5 ± 0.6
CD31	0.6 ± 0.4	1.6 ± 0.7	1.9 ± 0.3	1.2 ± 0.5
CD11b	0.2 ± 0.3	6.2 ± 10.7	18.5 ± 28.3	1.8 ± 1
CD45	20.7 ± 9.4	3.1 ± 3.9	2.1 ± 1.8	2.6 ± 1.5

characteristics.

3.2. AlClPc/NE

The choice of NE as a drug delivery system (DDS) should take in account analysis of the influence of the DDS on photophysical parameters of the system compared with its behaviour in a homogeneous solution and in micro heterogeneous systems. In addition to improving cellular uptake, the DDS should mimic most biological systems and be relatively safe (to have low toxicity). The absorption spectrum of AlClPc in an organic medium and in NE systems was typical of non-aggregated species (data not shown). The absorption spectra revealed the characteristic Soret band of PS (between 300 and 410 nm), which arises due to electronic transitions of the π-π* type. The spectra also contained a set of Q bands located between 630 and 740 nm. Fluorescence spectroscopy also mediated characterization of the photophysical properties of AlClPc incorporated into the DDS. There was a small Stokes shift in the fluorescence spectrum of AlClPc/NE when we compared its values in ethanol (674 nm) to those at 681 nm (incorporated into the NE system). This shift was associated with the ability of the DDS to stabilize the excited state of AlClPc. Therefore, the DDS used not significantly alter the absorption and fluorescence spectra of AlClPc.

The mean size distributions of the NE were determined by photon correlation spectroscopy using a Zetasizer Nano ZS from Malvern Instruments (Worcestershire). This method allows for determination of the mean diameter of particles (hydrodynamic radius), polydispersity index (PdI), and zeta potential of the particle population. The reported values were expressed as mean ± SD of at least three different batches of each formulation. Dynamic light scattering (DLS) analyses showed appropriate PdI values (< 0.3) for AlClPc/NE, which suggested a monodisperse distribution in the colloidal medium. The size and PdI were 178.0 nm (± 2.0) and 0.24, respectively, which were in agreement with previous reports on polymeric NEs and photosensitizers.

A previous study on AlClPc (free or incorporated into a DDS) described a stable second-generation photosensitizer drug with optimal wavelengths in 610–660 nm [25,26]. Our study showed that the photoactivation process induced BM-MSCs to differentiate into adipocytes by photo-induced biomodulation with LLL at a dose of 20 mJ/cm^2 in the presence of AlClPc/NE (5.0 µmol/L).

3.3. A high dose of AlClPc/NE is toxic for murine BM-MSCs

The MTT assay was conducted to assess the intrinsic cytotoxic effect of AlClPc/NE, and to evaluate the viability of BM-MSCs at various AlClPc/NE concentrations. The viability of control BM-MSCs was 100% (± 0.05%). Following incubation with AlClPc/NE at concentrations of 0.5, 1.0, 2.5, 5.0, and 7.5 µM, cell viability was maintained at approximately 99.2% (± 4.7%), 96.7% (± 4.5%), 94.7% (± 10.5%), 91.2% (± 8.5%), and 26.9% (± 3.1%) ($P < 0.05$), respectively (Fig. 2A). Cytotoxicity at doses of 0.5 and 1.0 µM was comparable to that of control cells; a dose of 7.5 µM AlClPc/NE resulted in significant reduction in BM-MSC viability. Since lower cytotoxic effects were observed with 2.5 and 5.0 µM AlClPc/NE relative to other doses, further photo-induced biostimulation experiments on AlClPc/NE were conducted at these doses to ensure safety.

3.4. Low photo-cytotoxic effects AlClPc/NE-LLL on BM-MSCs

To evaluate the potential effect of visible light at 660 nm, we applied a combination of AlClPc/NE and LLL to murine BM-MSCs, and examined photo-induced biomodulation via adipogenic differentiation assays *in vitro*. Twenty-four hours after treatment with 2.5 or 5.0 µM AlClPc/NE plus LLL at 40 or 20 mJ/cm^2, no statistically significant decrease ($P < 0.05$) in the percentage of viable cells was observed. The use of LLL in the absence of AlClPc/NE, as well as empty NE in the absence of LLL did not affect any of the parameters studied (data not shown). Consequently, these results revealed that a combination of 5.0 µM and 20 mJ/cm^2 is optimal for studying dipogenic differentiation by photo-biostimulation.

The MTT assay was performed 1–7 days after treatment with 5.0 µM AlClPc/NE, at a light dose of 20 mJ/cm^2 (AlClPc/NE-LLL), to evaluate the growth curve of BM-MSCs. With the same photosensitizer concentration and time of illumination, it was possible to maintain cell viability at approximately 99.2% (± 4.7%) on day 1, 96.7% (± 4.5%) on day 2, 94.7% (± 10.5%) on day 3, 91.2% (± 8.5%) on day 4, 26.9% (± 3.1%) on day 5, 26.9% (± 3.1%) on day 6, and 26.9% (± 3.1%) on day 7 ($p < 0.05$; Fig. 3 B). It was noted that in the control groups – LLL in the absence of AlClPc/NE and empty NE in the absence of LLL – cultured BM-MSCs showed similar growth curves as compared with that of control cells that did not receive any treatments (data not shown). Taken together, these results confirmed again that the combination of 5.0 µM AlClPc/NE and 20 mJ/cm^2 LLL is the most suitable for

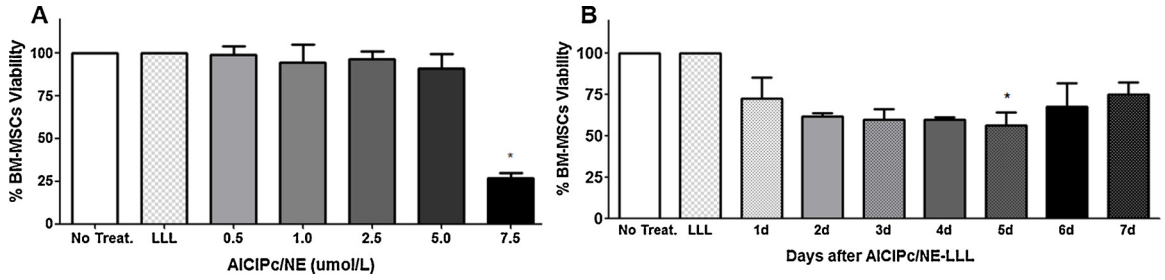

Fig. 2. Murine BM-MSCs proliferation, as analysed by the MTT assay. (A) High dose AlClPc/NE dose. Twenty-four hours after the nanoemulsion treatment, the MTT test was performed for cells viability with several doses of AlClPc/NE. (B) Growth curve of BM-MSCs treatment with 5.0 µM AlClPc/NE and at a light dose of 20 mJ/cm^2; MTT test was conducted every day during the one-week (Day 1–7) post-irradiation period. No treatment control group refer to BM-MSCs culture without any LLL or AlClPc/NE. LLL control group refers to BM-MSCs culture without AlClPc/NE. Values are expressed as mean ± SD of three samples. *p < 0.05 for experimental group related as compared to control groups.

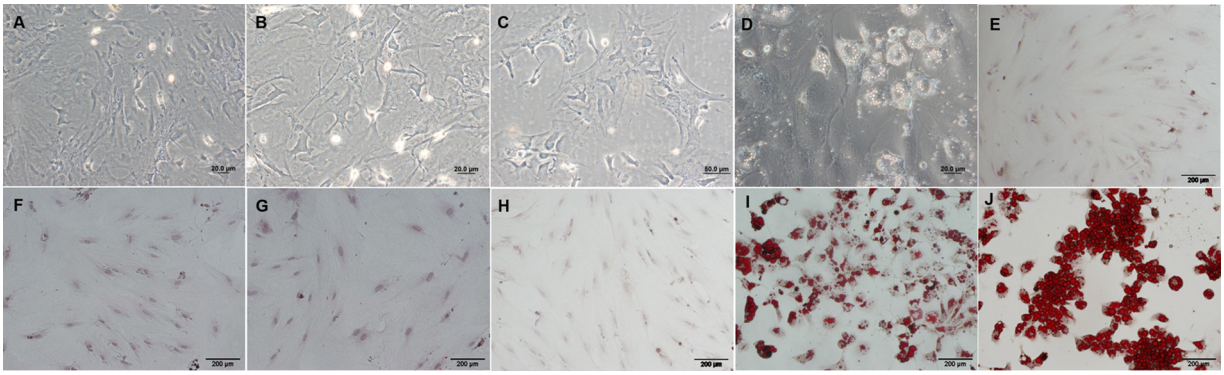

Fig. 3. Adipogenic differentiation of murine BM-MSCs induced by AlClPc/NE-LLL. All cell groups were cultured with α-MEM medium supplemented with 15% of FBS and were observed through an inverted phase-contrast microscope (panels A–D). Control cells groups were analysed by Sudan II/Scarlet staining: No treatment control cells (panel F), AlClPc/NE control cells (panel G), and LLL control cells (panel H). Adipogenic induction by AlClPc/NE-LLL was analysed by Sudan II/Scarlet staining of lipid vacuoles: Experimental group (panel I). No treatment control group refer to BM-MSCs culture without any treatment, AlClPc/NE control group refer to BM-MSCs that received only nanoemulsion containing AlClPc, LLL control group refer to BM-MSCs that received only low laser light, and Experimental group refer to BM-MSCs that received AlClPc/NE-LLL. Scale bars represent 20 μm (panels A, B and D), 50 μm (panel C) and 200 μm (panels E, F, G, H, I and J).

studying photo-induced biostimulation.

3.5. AlClPc/NE-LLL induces adipogenic differentiation of BM-MSCs

After primary culture in fresh medium and expansion to the fourth passage (Fig. 1F), BM-MSCs were subjected to phot-induced biomodulation for differentiation into adipocytes. The control and experimental BM-MSC groups were examined daily, and images were captured via phase contrast microscopy. Three days following the adipogenic AlClPc/NE-LLL induction protocol, we observed that experimental BM-MSCs exhibited changes in morphology; the elongated fibroblastic appearance was converted to a rounder shape. Five to six days after LLL irradiation of BM-MSCs pre-treated with AlClPc/NE, lipid-filled cells were observed (Fig. 3D). We noticed that the appearance of control BM-MSCs (no treatment, only AlClPc/NE, and LLL alone) did not undergo any morphological alterations (Fig. 3A–C).

Adipogenic characteristics were confirmed in the experimental BM-MSC group by positive Sudan II/Scarlet staining, which was used to assess acquisition of intracellular lipid droplets throughout the cell cytoplasm following induction of differentiation by AlClPc/NE-LLL (Fig. 3I). On the other hand, control BM-MSCs (no treatment, AlClPc/NE, and LLL) did not stain (Fig. 3F–H).

Expression levels of genes that are highly expressed in adipocytes were confirmed by qPCR in experimental murine BM-MSCs six days after AlClPc/NE-LLL stimulation. The expression of marker PPARγ was 11.8× higher in experimental (AlClPc/NE-LLL) BM-MSCs as compared with that in controls groups (Fig. 4A); expression of marker LPL was 9.3× higher in experimental (AlClPc/NE-LLL) BM-MSCs as compared with that in control groups (Fig. 4B). However, these markers were almost absent in control groups (Fig. 4A and B).

Next, we evaluated expression of mouse MSC surface markers six days after AlClPc/NE-LLL by flow cytometry. The experimental BM-MSC group expressed lower levels of murine BM-MSC markers such as CD73 (5.9% ± 6.1% of all cells), CD44 (10.9% ± 10.1%), CD117 (2.2% ± 0.6%), CD105 (2.8% ± 1.1%), and SCA1 (79.8% ± 17.6%) as compared with those of control groups (no treatment, AlClPc/NE, and LLL)(Table 2). The experimental BM-MSC group showed very low expression of classical hematopoietic markers CD45 (2.6% ± 1.5%), CD34 (1.5% ± 0.6%), and CD11b (1.8% ± 1%), as well as the classical endothelial marker CD31 (1.2% ± 0.5%; Table 2). Therefore, experimental BM-MSCs almost completely lost MSC characteristics.

3.6. Continuous GFP expression

In parallel, the visibility and intensity of GFP expression in murine BM-MSCs were evaluated in this study. Images obtained by fluorescence microscopy showed high expression of GFP in bone marrow cell culture at P2 (Fig. 5A), and this high expression seemed to have increased at P4 (Fig. 5B). Besides, fluorescence microscopy suggested that there was no significant decrease in GFP expression after adipogenic differentiation treatment of BM-MSCs with AlClPc/NE-LLL when compared with the control groups (data not shown). By flow cytometry, we observed that

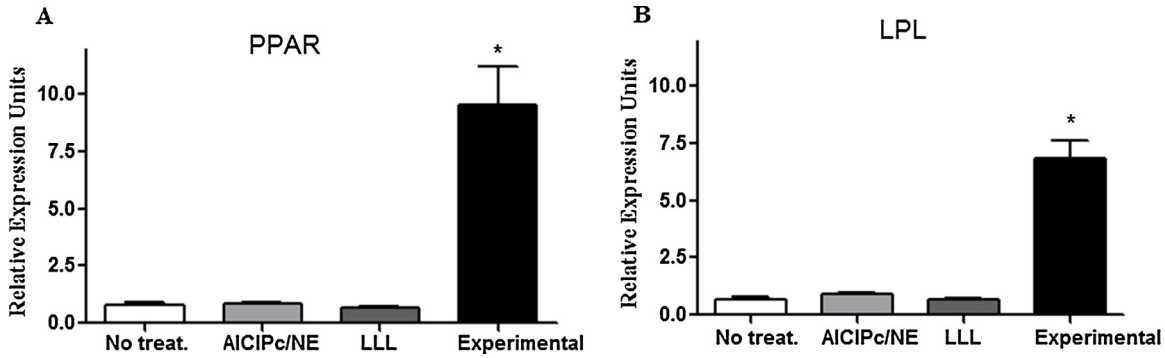

Fig. 4. BM-MSCs differentiated into adipocytes express transcripts associated with adipogenesis. Cellular differentiation induced by AlClPc/NE-LLL was analysed by mRNA expression of the PPARγ (A) and LPL genes (B) via qPCR. Gene expression was normalized relative to the reference gene GAPDH. No treatment control group refers to BM-MSCs culture without any treatment, AlClPc/NE control group refers to BM-MSCs that received only nanoemulsion containing AlClPc, LLL control group refers to BM-MSCs that received only low laser light therapy, and Experimental group refer to BM-MSCs that received AlClPc/NE-LLL. Results are expressed as mean ± SD of three samples, $p < 0.05$.

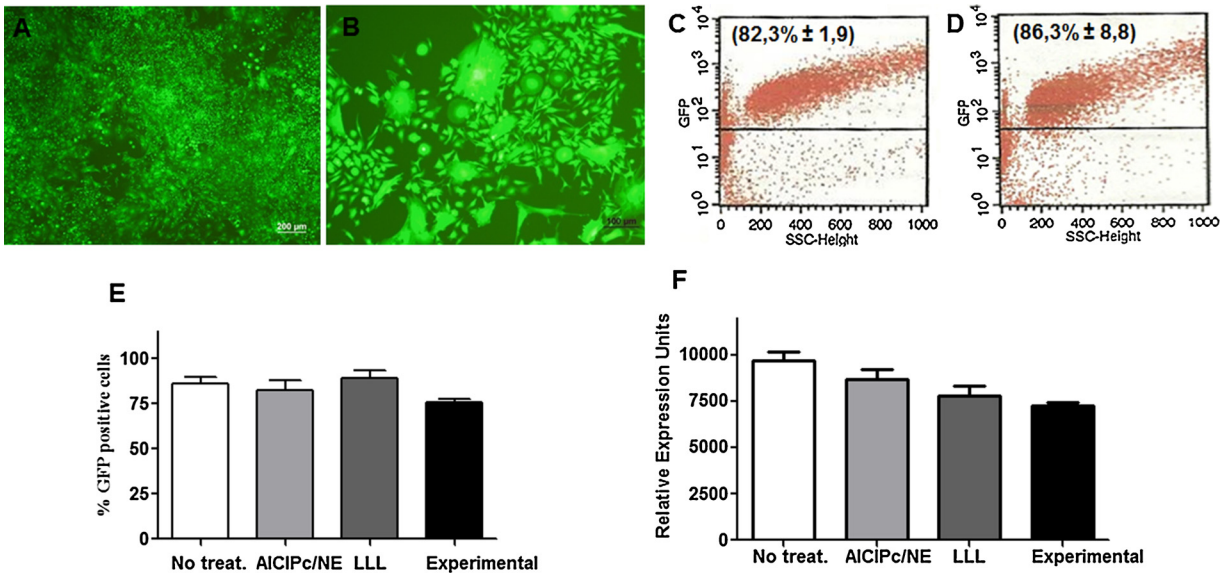

Fig. 5. Endogenous GFP expression level remained high in murine BM-MSCs after AlClPc/NE-LLL. Fluorescence microscopic images showing GFP expression in BM-MSCs at P2 (panel A) and P4 (panel B). Flow cytometry of cells marked with endogenous GFP protein at P2 (panel C) and at P4 (panel D). After photo-induced biomodulation at P4, all groups were analysed for percentage of cells expressing GFP protein (panel E). Comparative analyses of GFP mRNAs in all groups; gene expression was normalized relative to the reference gene GAPDH (panel F). No treatment control group refers to BM-MSCs culture without any treatment, AlClPc/NE control group refers to BM-MSCs that received only nanoemulsion containing AlClPc, LLL control group refers to BM-MSCs that received only low laser light therapy, and Experimental group refers to BM-MSCs that received AlClPc/NE-LLL. Results are expressed as mean ± SD of three samples, $p < 0.05$.

during the entire process of isolation and expansion of BM-MSCs, endogenous GFP expression was high; it was 82.3% (± 1.9%) at P2 (Fig. 5C) and 86.3% (± 8.8%) at P4 (Fig. 5D), without any statistically significant decrease. Following photo-induced biomodulation at P4, experimental (AlClPc/NE-LLL) BM-MSCs differentiated into adipocytes; high GFP expression was maintained (75.5% ± 5%; Fig. 5E). AlClPc/NE and LLL control cells expressed GFP at 82.3% (± 15.2%) and 89% (± 12.1%), respectively; these values were not significantly different from those in the experimental group (Fig. 5E). Moreover, qPCR analysis demonstrated that GFP expression was higher in control groups as compared with that in experimental groups: no treatment (9288.3 ± 141.4 relative expression units), AlClPc/NE (8701.3 ± 707.1 relative expression units), LLL (7783.2 ± 730.4 relative expression units), and experimental (7363.1 ± 184.9 relative expression units; Fig. 5F). Accordingly, GFP expression stayed high in all murine BM-MSC groups.

3.7. Experimental AlClPc/NE-LLL BM-MSCs do not induce tumorigenesis in vivo

To ensure that the experimental AlClPc/NE-LLL BM-MSCs group did not contain cells with abnormal proliferative characteristics, we examined their tumorigenic potential *in vivo*. After 21 days, tumour formation was not observed in C57BL/6-GFP$^+$ mice. Histopathological analysis showed absence of morphological changes in muscles of mice that received sc infusion of experimental BM-MSCs (Fig. 6D). These results indicated that the AlClPc/NE-LLL protocol is safe, and experimental AlClPc/NE-LLL BM-MSCs are free of cells capable of malignant transformation.

4. Discussion

In the present study, we showed that controlled release of a photosensitizer agent (AlClPc/NE) in combination with LLL can induce adipogenic differentiation of murine BM-MSCs via photo-induced biomodulation. We stably expressed GFP (as a transgene) as a marker, and visualized induction of intracellular lipid droplets throughout the cytoplasm and expression of adipogenic-differentiation markers. For this purpose, we isolated MSCs from murine bone marrow; these cells had morphological, immunophenotypic, and differentiation characteristics similar to those of BM-MSCs, as described by Friedenstein et al. (1970) [1]. Isolated murine BM-MSCs provided a fast, reliable, and low-cost method for studying adipogenic differentiation potential.

Adipogenically differentiated cells from BM-MSCs can be used to set up models of tissue regeneration and tissue engineering, and offers an alternative method for producing new autologous tissue [28]. In addition, adipose tissue engineering exhibits high potential for regenerative and aesthetic medicine, such as reconstruction of defective areas caused by trauma or cancer [29]. For these reasons, primary murine BM-MSCs were the most attractive sources of cells for our purposes.

Some researchers have stated that LLL therapy can stimulate MSC proliferation and growth of differentiated cells [30,31]. Kushibiki et al. (2015) showed that laser irradiation of MSCs directs their differentiation toward osteocytes and chondrocytes [32]. Primo et al. (2011) reported a photo-modulation process that stimulates BM-MSCs with LLL therapy and a therapeutic photosensitizer agent (AlClPc) encapsulated within polymeric NEs (AlClPc/NE) to induce wound healing [17]. On the other hand, the use of combination therapy using AlClPc/NE and LLL to induce adipogenic differentiation of murine BM-MSCs has not been previously studied.

Some studies indicate that age contributes significantly to bone marrow adipogenesis [33,34]. Ortin-Martinez et al. (2017) demonstrated that GFP from the jellyfish *Aequorea victoria* is a useful gene reporter in regenerative medicine studies [35]. Therefore, all our experiments were carried out with the fourth passage (P4) of homogeneously labelled BM-MSCs from GFP transgenic mice.

Cell growth curve of the experimental group showed only a slight decline in the proportion of viable cells, which continued to proliferate six days post photo-induced biomodulation with 5.0 μM AlClPc/NE and a 660-nm laser at 20 mJ/cm^2. Pogrel et al. (1997) have previously demonstrated that LLL does not induce proliferation of fibroblasts and keratinocytes *in vitro* [36]. Mvula et al. (2010) reported that LLL at 5 J/cm^2 and 636 nm, when applied to adult adipose tissue-derived stem cells (ADSCs) and combined with epidermal growth factor (EGFR) pretreatment, increases cellular viability and proliferation [30]. Moore et al. (2005) showed that primary fibroblasts proliferate effectively

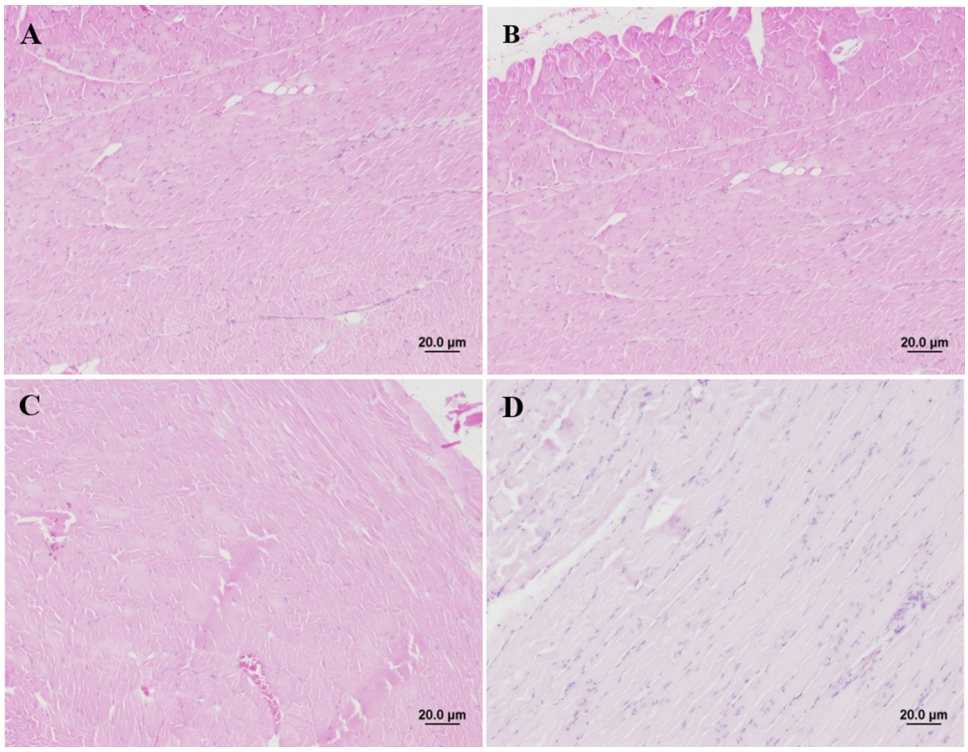

Fig. 6. Experimental AlClPc/NE-LLL BM-MSCs do not exhibit tumorigenesis potential in vivo. Treated and untreated murine BM-MSCs were subcutaneously (sc) infused into C57BL/6-GFP$^+$ mice, and the presence of tumour muscle tissue was analysed after 21 days. The H&E staining of control mouse tissue (panel A); control mouse tissue with sc infusion of PBS (1x) (panel B); control mouse tissue with sc infusion of untreated BM-MSCs (panel C); mouse tissue with sc infusion of differentiated BM-MSCs into adipocytes by AlClPc/NE-LLL (panel D). The scale bars represent 20 µm.

after irradiation at 665 and 675 nm, while 810-nm irradiation inhibited cell proliferation [37]. De Villiers et al. (2011) exposed ADSCs to 636-nm light at 5 J/cm^2 and observed increased cellular viability [38]. In general, irradiation in the range of 600–700 nm yielded satisfactory photo-induced biomodulation in MSCs [39,19,32].

To meet the criteria of the International Society for Cellular Therapy (ISCT) [40], we examined primary murine BM-MSCs, the AlClPc/NE control group, the LLL control group, and the experimental group, which were adipogenically differentiated BM-MSCs induced by AlClPc/NE-LLL. Morphological analysis showed that primary murine BM-MSCs and all control groups of cultured cells were adherent and exhibited spindle shape, which is typical of fibroblasts [41]. On the other hand, the experimental cell culture group contained lipid-filled cells six days after AlClPc/NE-LLL, thus confirming adipogenic differentiation.

Flow cytometric analyses showed that expression levels of MSC surface markers were considerably lower in the experimental group as compared with those in the control groups (no treatment, AlClPc/NE, and LLL). In addition, cells in all groups (control and experimental) lacked hematopoietic and endothelial markers; this was similar to findings by Karp et al. (2009) [49]. Our results suggested that cells in the experimental group were not closely related to either hematopoietic or endothelial lineages but expressed only 1.1-fold less SCA1 (MSC marker) when compared with the no-treatment group. In summary, cells in the experimental group lost almost all MSC characteristics after AlClPc/NE-LLL, which suggested that this group of cells differentiated into adipocytes.

In order to examine the molecular mechanisms in more detail, we evaluated the expression of adipogenesis marker genes. Our results revealed that adipogenic genes (at the mRNA level) that are usually expressed in pre-mature and mature adipocytes were also significantly up-regulated in our experimental group cells, especially six days post-cultivation. PPARγ is a nuclear receptor that is activated during adipogenic differentiation, and acts as a key transcriptional regulator of adipocytic conversion. Absence of PPARγ prevents precursor cells from differentiating into mature adipocytes [42,43]. Furthermore, PPARγ is expressed in stem cells and in more specific progenitor cells [48]. Therefore, we detected only basal levels of PPARγ in all our control groups.

It is known that the *LPL* gene participates in lipoprotein metabolism by breaking triglycerides (from a molecule of fatty acids) into chylomicron and very low-density lipoprotein (VLDL) to facilitate absorption of lipids [44]. *LPL* gene expression is observed mainly in mature adipocytes, and its transcription pattern depends on the stage of adipogenesis [45,42]. In line with these data, we confirmed increased LPL mRNA expression following AlClPc/NE-LLL treatment in our experimental group cells.

Similar to results from other studies [46,35,50], among murine BM-MSCs, we observed terminally differentiated cells with elevated GFP expression via flow cytometry and qPCR. This confirmed that photo-induced biomodulation by AlClPc/NE-LLL and adipogenic differentiation does not affect GFP expression. BM-MSCs with stably-expressed GFP (transgene) after treatment with AlClPc/NE-LLL seem to be an attractive source for research on tissue regeneration and tissue engineering *in vivo*.

Furthermore, MSCs have negligible immunogenicity; therefore, these cells are strong candidates for cell-based therapies [47]. We determined whether expression of endogenous GFP and differentiation into adipocytes by AlClPc/NE-LLL in murine BM-MSCs can generate tumours *in vivo*. In all treated mice, no significant histopathological changes were observed following the transplant, suggesting that the AlClPc/NE-LLL method is safe for *in vivo* studies.

In conclusion, we described characteristics of labelled BM-MSCs from GFP transgenic mice, and investigated the effects of AlClPc/NE alone, LLL alone, or combined AlClPc/NE-LLL in BM-MSCs. This is the first paper that describes a cellular photo induced biomodulation procedure that induces adipogenesis; this process was involves the combined treatment of a photosensitive agent (AlClPc/NE) with a low laser irradiation dose. Based on the results, we showed that cell therapy based on BM-MSCs and photo-induced biomodulation using AlClPc/NE-LLL may contribute to the development of new therapeutic strategies that are faster and more effective than traditional methods for regenerative medicine; the new upcoming protocol will be detailed in Tissue Engineering.

Fundings

This work was supported by Foundation for the State of São Paulo Research – FAPESP Thematic project # 2013/50181-1 A.C.T is also thankful to FINEP (project #01.10.0758.01) and CNPq-National Institute of Science and Technology-INCT of Nanobiotechnology (Project # 573880/2008-5) for the financial support.

Conflicts of interest

None.

References

[1] A.J. Friedenstein, R.K. Chailakhjan, K.S. Lalykina, The development of fibroblast colonies in monolayer cultures of guinea-pig bone marrow and spleen cells, Cell Tissue Kinet. 3 (4) (1970) 393–403.
[2] D.J. Prockop, Marrow stromal cells as stem cells for nonhematopoietic tissues, Science 276 (1997) 71–74.
[3] G. Rigotti, A. Marchi, M. Galiè, G. Baroni, D. Benati, M. Krampera, A. Pasini, A. Sbarbati, Clinical treatment of radiotherapy tissue damage by lipoaspirate transplant: a healing process mediated by adipose-derived adult stem cells, Plast. Reconstr. Surg. 119 (2007) 1409–1422.
[4] P.K. Mishra, Bone marrow-derived mesenchymal stem cells for treatment of heart failure: is it all paracrine actions and immunomodulation? J. Cardiovasc. Med. 9 (2008) 122–128.
[5] K. Le Blanc, C. Tammik, K. Rosendahl, E. Zetterberg, O. Ringdén, HLA expression and immunologic properties of differentiated and undifferentiated mesenchymal stem cells, Exp. Hematol. 31 (2003) 890–896.
[6] G.C. Reilly, A.J. Engler, Intrinsic extracellular matrix properties regulate stem cell differentiation, J. Biomech. 43 (2010) 55–62.
[7] A.G. Cristancho, M.A. Lazar, Forming functional fat: a growing understanding of adipocyte differentiation, Nat. Rev. Mol. Cell Biol. 28 (2011) 722–734.
[8] L.C. Clauser, R. Tieghi, M. Galiè, F. Carinci, Structural fat grafting: facial volumetric restoration in complex reconstructive surgery, J. Craniofac. Surg. 22 (2011) 1695–1701.
[9] F. Martins de Carvalho, D. Casal, J. Bexiga, J. Sousa, J. Martins, E. Teófilo, F. Maltez, I. Germano, E. Videira, J. Castro, HIV-associated facial lipodystrophy: experience of a tertiary referral center with fat and dermis-fat compound graft transfer, Eplasty 16 (2016) e31.
[10] M.P. Rowan, L.C. Cancio, E.A. Elster, D.M. Burmeister, L.F. Rose, S. Natesan, R.K. Chan, R.J. Christy, K.K. Chung, Burn wound healing and treatment: review and advancements, Crit. Care 19 (2015) 243.
[11] A. Crous, H. Abrahamse, Low-intensity laser irradiation at 636 nm induces increased viability and proliferation in isolated lung cancer stem cells, Photomed. Laser Surg. 34 (2016) 525–532.
[12] R.O. Poyton, K.A. Ball, Therapeutic photobiomodulation: nitric oxide and a novel function of mitochondrial cytochrome c oxidase, Discov. Med. 11 (2011) 154–159.
[13] C. Edmonds, S. Hagan, S.M. Gallagher-Colombo, T.M. Busch, K.A. Cengel, Photodynamic therapy activated signaling from epidermal growth factor receptor and STAT3: targeting survival pathways to increase PDT efficacy in ovarian and lung cancer, Cancer Biol. Ther. 13 (2012) 1463–1470.
[14] W.Y. Chu, M.H. Tsai, C.L. Peng, Y.H. Shih, T.Y. Luo, S.J. Yang, M.J. Shieh, pH-responsive nanophotosensitizer for an enhanced photodynamic therapy of colorectal cancer overexpressing EGFR, Mol. Pharm. 15 (2018) 1432–1444.
[15] L. Abramovitch-Gottlib, T. Gross, D. Naveh, S. Geresh, S. Rosenwaks, I. Bar, R. Vago, Low level laser irradiation stimulates osteogenic phenotype of mesenchymal stem cells seeded on a three-dimensional biomatrix, Lasers Med. Sci. 20 (2005) 138–146.
[16] L.F. de Freitas, M.R. Hamblin, Proposed mechanisms of photobiomodulation or low-level light therapy, IEEE J. Sel. Top. Quant. Electron. 22 (2016) 3.
[17] F.L. Primo, M.B. da Costa Reis, M.A. Porcionatto, A.C. Tedesco, *In vitro* evaluation of chloroaluminum phthalocyanine nanoemulsion and low-level laser therapy on human skin dermal equivalents and bone marrow mesenchymal stem cells, Curr. Med. Chem. 18 (2011) 3376–3381.
[18] L.P. Franchi, C.F. Amantino, M.T. Melo, A.P. de Lima Montaldi, F.L. Primo, A.C. Tedesco, *In vitro* effects of photodynamic therapy induced by chloroaluminum phthalocyanine nanoemulsion, Photodiagn. Photodyn. Ther. 6 (2016) 100–105.
[19] T. Kushibiki, T. Hirasawa, S. Okawa, M. Ishihara, Low reactive level laser therapy for mesenchymal stromal cells therapies, Stem Cells Int. 2 (2015) 974864.
[20] D.C. Zancanela, F.L. Primo, A.L. Rosa, P. Ciancaglini, A.C. Tedesco, The effect of photosensitizer drugs and light stimulation on osteoblast growth, Photomed. Laser Surg. 10 (2011) 699–705.
[21] F.L. Primo, M.M. Rodrigues, A.R. Simioni, Z.G. Lacava, P.C. Morais, A.C. Tedesco, Photosensitizer-loaded magnetic nanoemulsion for use in synergic photodynamic and magnetohyperthermia therapies of neoplastic cells, J. Nanosci. Nanotechnol. 8 (2008) 5873–5877.
[22] E.S. Tabosa do Egito, H. Fessi, M. Appel, F. Puisieux, J. Bolard, J.P.H. Devissaguet, New techniques for preparing submicronic emulsion: application to amphotericin, B. STP Pharma Sci. 4 (1994) 155–162.
[23] F. Denizot, R. Lang, Rapid colorimetric assay for cell growth and survival. Modifications to the tetrazolium dye procedure giving improved sensitivity and reliability, J. Immunol. Methods 89 (1986) 271–277.
[24] E. Albesiano, B.T. Messmer, R.N. Damle, S.L. Allen, K.R. Rai, N. Chiorazzi, Activation-induced cytidine deaminase in chronic lymphocytic leukemia B cells: expression as multiple forms in a dynamic, variably sized fraction of the clone, Blood 102 (2003) 3333–3339.
[25] I.R. Calori, A.C. Tedesco, Lipid vesicles loading aluminum phthalocyanine chloride: formulation properties and disaggregation upon intracellular delivery, J. Photochem. Photobiol. B 160 (2016) 240–247.
[26] K.R. Py-Daniel, J.S. Namban, L.R. de Andrade, L.G. PE de Souza, R.B. Paterno, M.A.Soler Azevedo, Highly efficient photodynamic therapy colloidal system based on chloroaluminum phthalocyanine/pluronic micelles, Eur. J. Pharm. Biopharm. 103 (2016) 23–31.
[27] S.A. Bustin, V. Benes, J.A. Garson, J. Hellemans, J. Huggett, M. Kubista, R. Mueller, T. Nolan, M.W. Pfaffl, G.L. Shipley, J. Vandesompele, C.T. Wittwer, The MIQE guidelines: minimum information for publication of quantitative real-time PCR experiments, Clin. Chem. 55 (2009) 611–622.
[28] Z. Lu, Y. Yuan, J. Gao, F. Lu, Adipose tissue extract promotes adipose tissue regeneration in an adipose tissue engineering chamber model, Cell Tissue Res. 364 (2016) 289–298.
[29] Y. Yuan, J. Gao, R. Ogawa, Mechanobiology and mechanotherapy of adipose tissue-effect of mechanical force on fat tissue engineering, Plast. Reconstr. Surg. Glob. Open 7 (2016) e578.
[30] B. Mvula, T.J. Moore, H. Abrahamse, Effect of low-level laser irradiation and epidermal growth factor on adult human adipose-derived stem cells, Lasers Med. Sci. 25 (2010) 33–39.
[31] H. Tuby, L. Maltz, U. Oron, Low-level laser irradiation (LLLI) promotes proliferation of mesenchymal and cardiac stem cells in culture, Lasers Surg. Med. 39 (2007) 373–378.
[32] T. Kushibiki, Y. Tu, A.O. Abu-Yousif, T. Hasan, Photodynamic activation as a molecular switch to promote osteoblast cell differentiation via AP-1 activation, Sci. Rep. 5 (2015) 13114.
[33] A.C. Maurin, Chavassieux PM, L. Frappart, P.D. Delmas, C.M. Serre, P.J. Meunier, Influence of mature adipocytes on osteoblast proliferation in human primary co-cultures, Bone 26 (2000) 485–489.
[34] A. Wilson, H.Yu LA Shehadeh, K.A. Webster, Age-related molecular genetic changes of murine bone marrow mesenchymal stem cells, BMC Genomics 7 (2010) 229.
[35] A. Ortin-Martinez, E.L. Tsai, P.E. Nickerson, M. Bergeret, Y. Lu, S. Smiley, L. Comanita, V.A. Wallace, A reinterpretation of cell transplantation: GFP transfer from donor to host photoreceptors, Stem Cells 35 (2017) 932–939.
[36] M.A. Pogrel, J.W. Chen, K. Zhang, Effects of low-energy gallium-aluminum-arsenide laser irradiation on cultured fibroblasts and keratinocytes, Lasers Surg. Med. Suppl. 20 (1997) 426–432.
[37] P. Moore, T.D. Ridgway, R.G. Higbee, E.W. Howard, M.D. Lucroy, Effect of wavelength on low-intensity laser irradiation stimulated cell proliferation in vitro, Lasers Surg. Med. 36 (2005) 8–12.
[38] J.A. De Villiers, N.N. Houreld, H. Abrahamse, Influence of low intensity laser irradiation on isolated human adipose derived stem cells over 72 hours and their differentiation potential into smooth muscle cells using retinoic acid, Stem Cell Rev. 7 (2011) 869882.
[39] R. Fekrazad, S. Asefi, M. Allahdadi, K.A. Kalhori, Effect of photobiomodulation on mesenchymal stem cells, Photomed. Laser Surg. 34 (2016) 533–542.
[40] M. Dominici, K. Le Blanc, I. Mueller, I. Slaper-Cortenbach, F. Marini, D. Krause, R. Deans, A. Keating, Prockop DJ, E. Horwitz, Minimal criteria for defining multipotent mesenchymal stromal cells. The International Society for Cellular Therapy position statement, Cytotherapy. 8 (2006) 315–317.
[41] D.T. Covas, R.A. Panepucci, A.M. Fontes, W.A. Silva Jr., M.D. Orellana, M.C. Freitas, L. Neder, A.R. Santos, L.C. Peres, M.C. Jamur, M.A. Zago, Multipotent mesenchymal stromal cells obtained from diverse human tissues share functional properties and gene-expression profile with CD146+ perivascular cells and fibroblasts, Exp. Hematol. 36 (2008) 642–654.
[42] D. Moseti, A. Regassa, W.K. Kim, Molecular regulation of adipogenesis and potential anti-adipogenic bioactive molecules, Int. J. Mol. Sci. 17 (2016) E124.
[43] I. Takada, A.P. Kouzmenko, S. Kato, PPAR-γ signaling crosstalk in mesenchymal stem cells, PPAR Res. (2010) 341671.
[44] P.L. Mok, S.K. Cheong, C.F. Leong, *In-vitro* differentiation study on isolated human mesenchymal stem cells, Malays. J. Pathol. 30 (2008) 11–19.
[45] H. Lu, L. Guo, M.J. Wozniak, N. Kawazoe, T. Tateishi, X. Zhang, G. Chen, Effect of cell density on adipogenic differentiation of mesenchymal stem cells, Biochem. Biophys. Res. Commun. 381 (2009) 322–327.
[46] Z. Ding, X. Liu, X. Ren, Q. Zhang, T. Zhang, Q. Qian, W. Liu, C. Jiang, Galectin-1-induced skeletal muscle cell differentiation of mesenchymal stem cells seeded on an acellular dermal matrix improves injured anal sphincter, Discov. Med. 117 (2016) 331–340.
[47] Trohatou, M.G. Roubelakis, Mesenchymal stem/stromal cells in regenerative medicine: past, present, and future, Cell. Reprogram. 4 (2017) 217–224.
[48] M. Kawai, Sousa KM, O.A. MacDougald, C.J. Rosen, The many facets of PPARγ: novel insights for the skeleton, Am. J. Physiol. Endocrinol. Metab. 99 (2010) E3–E9.
[49] J.M. Karp, G.S. Leng Teo, Mesenchymal stem cell homing: the devil is in the details, Cell Stem Cell 4 (2009) 206–216.
[50] R. Ogawa, M. Mizuno, A. Watanabe, M. Migita, H. Hyakusoku, T. Shimada, Adipogenic differentiation by adipose-derived stem cells harvested from GFP transgenic mice-including relationship of sex differences, Biochem. Biophys. Res. Commun. 319 (2004) 511–517.